Crystal Structure, Infrared, and Polarized Raman Spectra of $K_3Sm(PO_4)_2$

Mohamed Toumi,[a] Leila Smiri-Dogguy,[a] and Alain Bulou*[b]

Keywords: Phosphates / Structure / IR spectroscopy / Raman spectroscopy

The low-temperature form of $K_3Sm(PO_4)_2$ crystallizes in the monoclinic system [a = 7.4347(5) Å, b = 5.6270(5) Å, c = 9.4919(5) Å, β = 90.870(6)°, Z = 2, space group $P2_1/m$]. The structure has been determined using 1263 independent reflections (R = 0.045, R_w = 0.11) and is found to be of the glaserite type. The Raman and infrared spectra have been investigated: they are consistent with the proposed space group and an assignment of the observed frequencies is given.

Introduction

Compounds of the type $A_3M(TO_4)_2$ (M = Sc, Fe, Cr, rare earth; A = Na, K; T = P, V, As, S)[1−11] have structures built-up of isolated tetrahedra linked only by cations and exhibit pseudohexagonal symmetries. Their structures can be related to that of glaserite, $K_3Na(SO_4)_2$, which exhibits an ideal highly symmetrical arrangement (trigonal, $P\bar{3}\,m1$ space group, Z = 1, with a_0 = 5.547 Å c_0 = 7.070 Å in a hexagonal cell).[12] The latter consists of tetrahedral units separated by cavities, which are occupied by two kinds of atomic sequences (denoted E1 and E2) extending parallel to the c_0 axis. The E1 sequence involves potassium and sodium ions with coordination numbers of 12 and 6, respectively, while the E2 sequence involves ten-coordinated potassium ions.

In this work, we describe a new compound belonging to this structural family, namely $K_3Sm(PO_4)_2$. Such systems offer the possibility of doping by various rare earth ions, the luminescent properties of which can be useful in the field of lasers. The experimental conditions of preparation are given, along with details of the X-ray diffraction structure determination and the results of infrared and Raman investigations.

Results and Discussion

Structural Description and Discussion

Figure 1 shows a projection of the crystal structure in the [100] plane.[13] This arrangement is characterized by the presence of isolated $P(1)O_4$ and $P(2)O_4$ tetrahedra linked only by cations. All PO_4 tetrahedra have a mirror plane (a,c) and present a face almost parallel to the (b,c) plane.

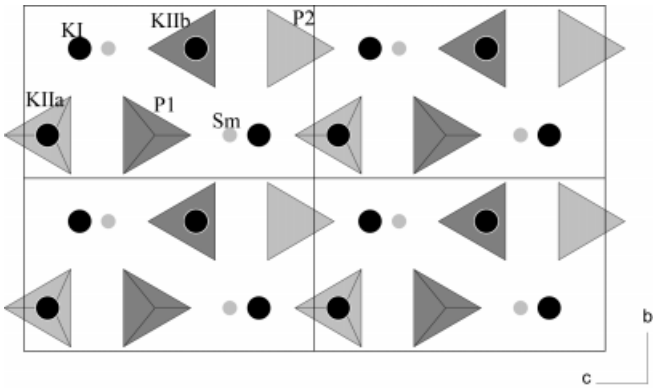

Figure 1. Projection of the $K_3Sm(PO_4)_2$ structure in the [001] plane

$P(1)O_4$ Tetrahedra: The average P(1)−O distance in the tetrahedra (1.542 Å; values range from 1.532 to 1.548 Å) is in good agreement with the value of 1.539 Å calculated by Baur and Khan.[14] The variance in the O−P−O bond angles, σ_1^2 = 2.37, is, however, larger than the value of 0.109 observed in $K_3Na(SO_4)_2$ [the variance σ^2 is defined as $\sigma^2 = 1/6\ \Sigma(\theta_i - 109.47)^2$, where θ_i represents the O−P−O bond angle and 109.47° is the ideal O−P−O bond angle in the PO_4 tetrahedron].

$P(2)O_4$ Tetrahedra: Again, the average P(2)−O distance (1.539 Å; range from 1.513 to 1.552 Å) is in good agreement with the calculated value. The variance σ_2^2 = 1.07 is much smaller than σ_1^2. The short P(2)−O(5) distance (1.513 Å) relates to the oxygen only bonded to potassium ions.

This structure can be described as comprising two types of sequences of atoms extending parallel to the a axis. The first sequence (E1) is formed by a regular succession of isolated PO_4 tetrahedra and potassium ions K(IIa) and K(IIb). The coordination numbers of K(IIa) and K(IIb) are 10 and 11, respectively. The second sequence (E2) consists of a regular succession of samarium and potassium ions. The coordination numbers are seven for samarium ions and nine for the potassium ions [K(I)].

The relationship between the $K_3Na(SO_4)_2$, β-K_2SO_4,[15] and $K_3Sm(PO_4)_2$ structures can easily be established by

[a] Laboratoire de Chimie Inorganique et Structurale, Faculté des Sciences de Bizerte,
7021 Zarzouna, Tunisia
[b] Laboratoire de Physique de l'Etat Condensé, UPRES-A CNRS no. 6087, Faculté des Sciences, Université du Maine,
F-72085 Le Mans Cedex 09, France

  1434−1948/99/0909−1545 $ 17.50+.50/0

considering the coordination numbers (given in square parentheses) and the cell parameters:

$K_3Na(SO_4)_2$	$[K^{[12]}Na^{[6]}][K^{[10]}(SO)_4]_2$	(a_0, c_0, $P\bar{3}$ $m1$)
β-K_2SO_4	$[K^{[9]}K^{[9]}][K^{[10]}(SO_4)]_2$	($a = c_0$; $b = a_0\sqrt{3}$; $c = a_0$; *Pnma*
$K_3Sm(PO_4)_2$	$[K^{[9]}Sm^{[7]}][K^{[10]}(PO)_4]$-$[K^{[11]}(PO_4)]$	($a = c_0$; $b = a_0$; c = $a_0\sqrt{3}$; β = 90.870°; $P2_1/m$)

The structure of β-K_2SO_4 is derived from the glaserite type through a reorientation of the tetrahedra as well as a disordering of the K^+ ions of the E2 sequence. The structure of $K_3Sm(PO_4)_2$ is similar to this β-K_2SO_4 arrangement, with only a slight distortion. The variation in the coordination numbers of the cations can be attributed to a slight rotation and distortion of PO_4 tetrahedra.

The greater distortion of $P(1)O_4$ compared to that of $P(2)O_4$ may be explained by considering the nearest neighbors: in the former case, only three samarium and four potassium ions are found at distances less than 3.6 Å, while seven potassium ions are present in the latter case.

Spectroscopic Analysis

Group Theory Analysis

In accordance with the space group $P2_1/m$, the normal modes of vibration can be classified in the following irreducible representations of C_{2h} as:

$\Gamma_{optic} = 26A_g + 16B_g + 15A_u + 24B_u$

$\Gamma_{acoustic} = 1A_u + 2B_u$.

The A_g and B_g modes are Raman-active, while the A_u and B_u modes are infrared (IR)-active.

Vibrations of the PO_4 Groups

The free PO_4^{3-} tetrahedron exhibits T_d symmetry and so possesses four normal modes of vibration having A_1 (ν_1 mode), E (ν_2) and F_2 (ν_3 and ν_4) symmetries with average wave numbers of 938, 420, 1017, and 567 cm^{-1}, respectively.[16] All of these modes are Raman active, whereas only the triply-degenerate ν_3 and ν_4 modes are IR-active. The ν_1 and ν_2 modes represent the symmetric stretching and deformation vibrations, while ν_3 and ν_4 represent the corresponding asymmetric stretching and deformation vibrations. Since the other PO_4^{3-} ions occupy sites of lower symmetry than that of the free ion, anisotropic crystal fields may remove degeneracies in the normal modes and allow inactive modes to become active.

In the crystal cell, the two PO_4^{3-} ions occupy C_s-symmetric sites. The site method[17] can be applied in the analysis of the internal modes of the PO_4 groups. Table 1 shows the correlation diagram between the free PO_4^{3-} group vibrations in T_d symmetry and the lattice PO_4^{3-} internal vibrations in C_{2h} symmetry through the C_s symmetry of one PO_4 in the crystal. The correlation shows that 18 Raman and 18 IR lines are predicted:

Raman:
8 stretching modes: 2 ν_1 ($2A_g$); 6 ν_3 ($4A_g$, $2B_g$)
10 deformation modes: 4 ν_2 ($2A_g$, $2B_g$); 6 ν_4 ($4A_g$, $2B_g$)
IR:
8 stretching modes: 2 ν_1 ($2B_u$); 6 ν_3 ($4B_u$, $2A_u$)
10 deformation modes: 4 ν_2 ($2A_u$, $2B_u$); 6 ν_4 ($4B_u$, $2A_u$)

Table 1. Correlation scheme for the internal vibrations of the PO_4 group

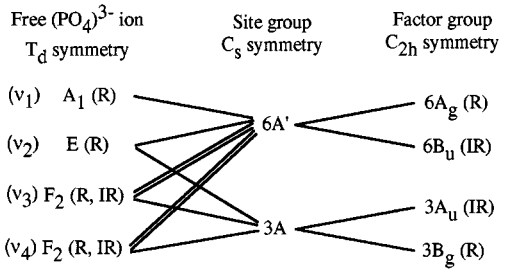

Analysis of IR Spectra

In view of the paucity of infrared data in the frequency range below 300 cm^{-1}, only assignment of the internal modes of the PO_4 will be discussed.

In the IR spectrum (Figure 2) the bands in the 970−1100 cm^{-1} region can be assigned to the asymmetric stretching (ν_3) mode.

The two nondegenerate symmetric stretching (ν_1) modes, observed at 936 and 964 cm^{-1}, confirm the presence of two crystallographically distinct PO_4 groups. The IR bands are strongly influenced by the cation environments.

Only three bands are observed (410, 414, and 466 cm^{-1}) for the doubly-degenerate symmetric bending (ν_2).

The triply-degenerate asymmetric bending mode (ν_4) gives four bands at 545, 574, 585, and 601 cm^{-1}.

Analysis of Raman Spectra:

According to group theory analysis, of the 81 optical modes, 42 are Raman-active. With reference to the Raman tensors (Table 2), they can be distinguished by polarization investigations.

Polarized Raman spectra were recorded for different orientations of the crystal. The A_g modes were obtained in the $z(xx)\bar{z}$, $z(yy)\bar{z}$, $y(zz)\bar{y}$, and $y(zx)\bar{y}$ geometries, the B_g modes in the $x(zy)\bar{x}$ and $z(xy)\bar{z}$ geometries. The spectra are shown in Figure 3.

PO_4 Vibrations

A_g Modes

The two high-intensity bands at 938 and 970 cm^{-1} can be assigned to A_g components of the nondegenerate ν_1 mode corresponding to phosphates in sites 1 and 2.

Group theory analysis predicts four bands for the asymmetric bending mode ν_3 (A_g). Four bands at 989, 1026, 1050, and 1100 cm^{-1} are indeed observed for this mode in the $z(xx)\bar{z}$, $z(yy)\bar{z}$, and $y(zx)\bar{y}$ orientations of the Raman

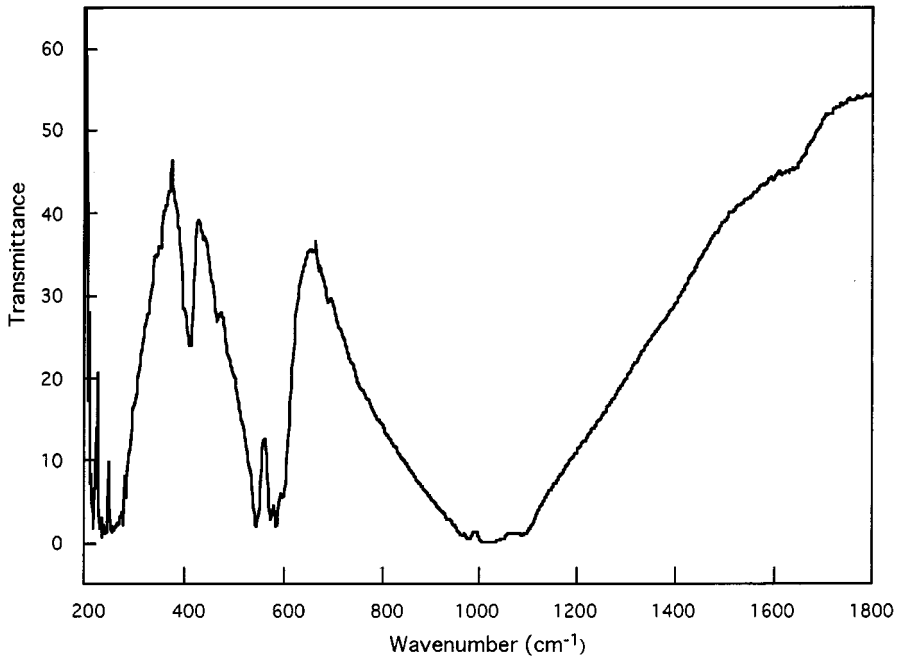

Figure 2. Infrared spectra of $K_3Sm(PO_4)_2$

Table 2. Raman tensors for the C_{2h} point group

	xx	0	*zx*		0	*yx*	0
A_g	0 xz	yy 0	0 zz	B_g	xy 0	0 yz	zy 0

spectra. In the $y(zz)\bar{y}$ orientation, only three bands at 989, 1050, and 1101 cm^{-1} are visible.

The polarized Raman bands observed at 561, 572, 589, and 609 cm^{-1} in the $z(xx)\bar{z}$, $z(yy)\bar{z}$, and $y(zz)\bar{y}$ spectra correspond to the asymmetric bending ν_4 (A_g) vibrations of the PO_4 group.

Factor group analysis predicts two bands for the symmetric bending ν_2 (A_g). Two bands at 415 and 450 cm^{-1} are indeed observed for this mode in the $z(yy)\bar{z}$ and $y(zx)\bar{y}$ orientations. In the $z(xx)\bar{z}$ and $y(zz)\bar{y}$ orientations, only one band at 450 cm^{-1} is seen.

B_g Modes

In the $x(zy)\bar{x}$ and $z(xy)\bar{z}$ geometries, 9 and 11 bands are observed, respectively.

$x(zy)\bar{x}$ 425, (450), 562, (572), (589), (938), (973), (988), 1009.

$z(xy)\bar{z}$ (416), 425, 447, 563, (573), 578, (589), (938), (972), (989), 1007.

According to group theory, only six lines are to be expected. In fact, detailed analysis shows that several lines correspond to A_g lines (frequencies in parentheses) and can be attributed to a contaminant that is difficult to completely eliminate for measurements under a microscope.

The bands at 425 and 447 cm^{-1} can be assigned to the $\nu_2(B_g)$ symmetric bending mode, those at 563 and 578 cm^{-1} to the $\nu_4(B_g)$ asymmetric bending mode, and those at 1007 and 1009 cm^{-1} to $\nu_3(B_g)$, the asymmetric bending mode.

In conclusion, the number of internal modes of the PO_4^{3-} anion observed in the Raman and IR spectra is consistent with predictions based on the proposed space group. The loss of symmetry compared to $K_3Na(SO_4)_2$[18] is clearly evident since the D_{3d} space group would lead to a much smaller number of Raman lines (Table 3).

External Modes

14 A_g and 10 B_g lines can be expected in the Raman low-frequency range, corresponding to external modes. In the absence of coupling, they would result from:

12 modes ($6A_g$ and $6B_g$) associated with the vibrations and translations of the PO_4 tetrahedra;

6 translational modes ($4A_g$ and $2B_g$) due to K^+ in K(IIa) and K(IIb) sites;

3 translational modes ($2A_g$ and $1B_g$) due to K^+ in a K(I) site;

3 translational modes ($2A_g$ and $1B_g$) due to Sm^{3+}.

Experimentally, 14 A_g modes and 10 B_g modes are indeed observed at the following wave numbers (cm^{-1}):

A_g mode: 73, 111, 121, 137, 151, 153, 161, 164, 179, 194, 209, 210, 228, 231,

B_g mode: 74, 82, 98, 126, 150, 165, 177, 188, 211, 234.

These modes are, as expected, well out of the frequency range of the internal modes of PO_4. However, it is very difficult to make assignments since the frequencies are al-

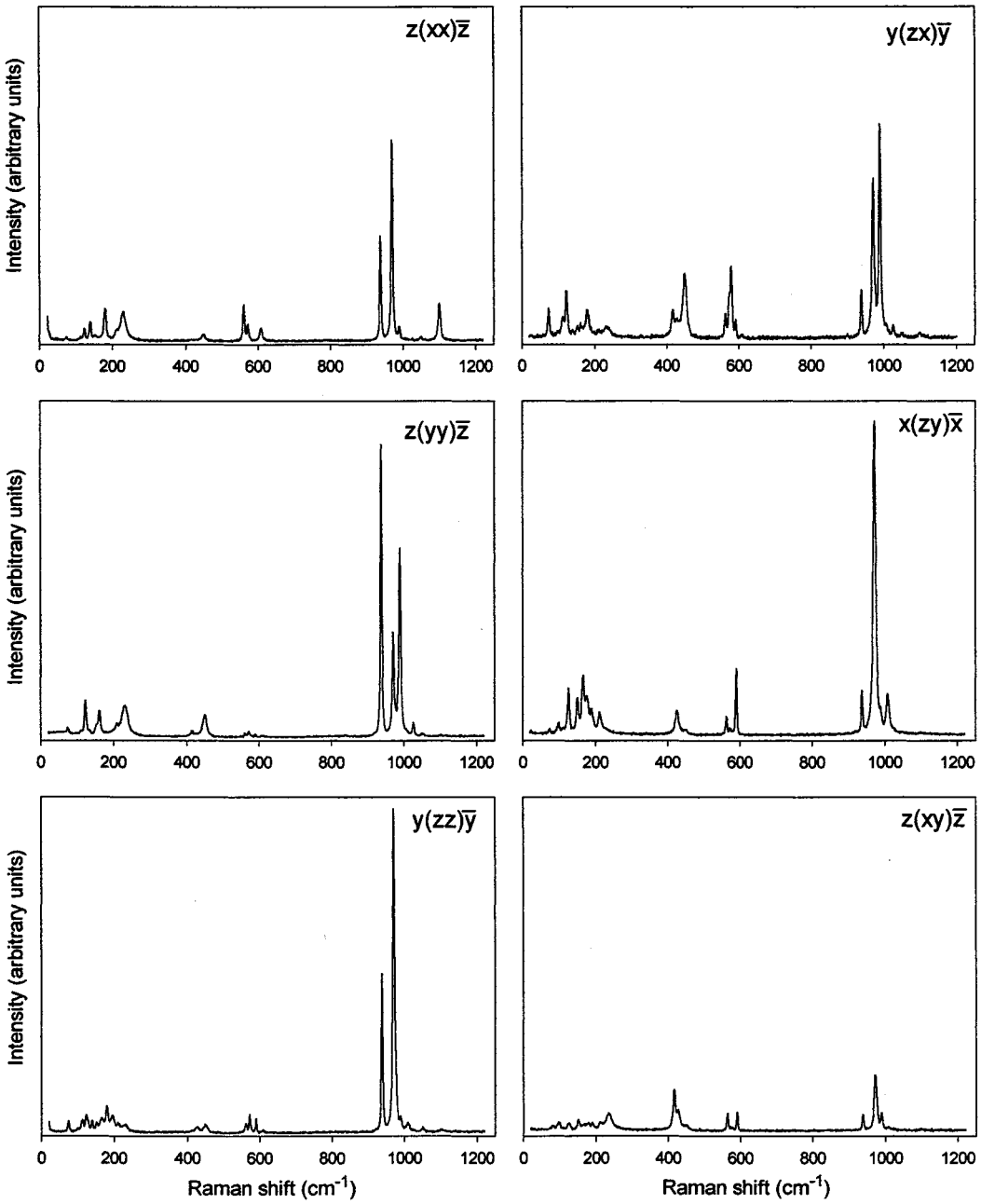

Figure 3. Raman spectra of $K_3Sm(PO_4)_2$ recorded in the various geometries indicated at the top right of each plot (the spectra recorded in cross-polarization mode are plotted with double scale)

most regularly spread and the various ionic displacements are presumably strongly coupled. Moreover, the compounds derived from glaserite[19] (space group $P\bar{3}\,m1$, $Z = 1$) that have so far been subjected to vibrational investigations,[20] such as $M^IM^{III}(XO_4)_2$ (M^I = K, Rb, Cs; M^{III} = In, Sc; X = Mo, W), do not possess the same ionic charges as in the present compound, neither for the cations nor for the molecular ions. Thus, it is not possible to extrapolate the frequencies merely from mass effects. A similar problem arises in the case of the Nasicon-type compounds Na_2-$M^{IV}(PO_4)_2$ (M^{IV} = Ti, Zr, Hf), also derived from glaserite, since the charge on samarium is just 3. However, with regard to the investigations of Barj et al.,[21] who assigned the translational modes of Ti, Zr, and Hf [setting on the K(I) site] at 195, 150, and 105 cm^{-1}, the modes involving samarium, with a lower charge, can be expected to appear at a lower frequency than 115 cm^{-1}. Indeed, several modes appear in this frequency range.

Conclusion

The crystal structure of $K_3Sm(PO_4)_2$ has been determined from single-crystal X-ray diffraction data. This structure is a derivative of the glaserite type.

Table 3. Relationship between the normal modes of vibration of the free PO_4 ions (center), those of $K_3Sm(PO_4)_2$ in the real $P2_1/m$ space (right), and those in the case of the ideal highly symmetrical glaserite (left)

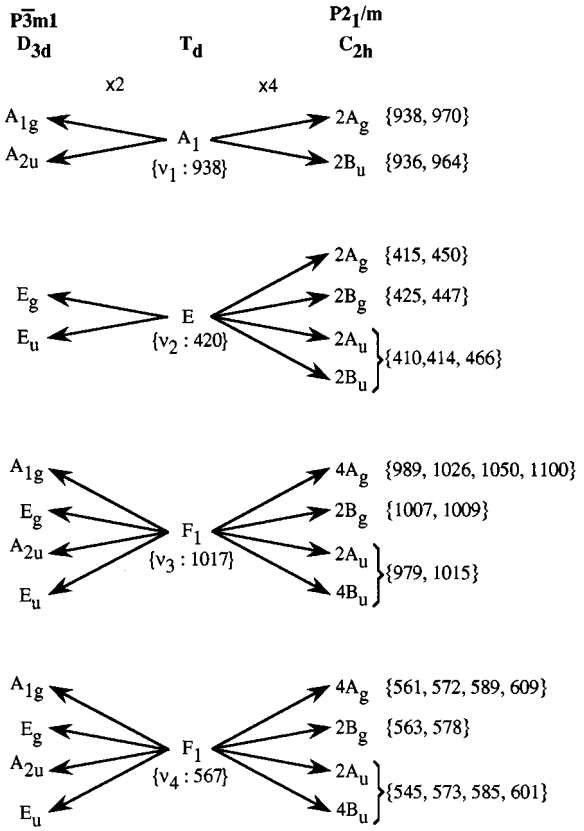

The infrared and Raman spectra of single crystals of $K_3Sm(PO_4)_2$ have been measured and studied in detail on the basis of group theory analysis and by reference to other compounds derived from glaserite. The internal vibrations of the PO_4^{3-} anion could all be identified. The Raman and infrared spectra confirm the structural distortions deduced from the X-ray diffraction study.

Table 4. Crystallographic characteristics, measurement and refinement conditions for $K_3Sm(PO_4)_2$

Crystal data	
Chemical formula	$K_3Sm(PO_4)_2$
Crystal system	Monoclinic
Space group	$P2_1/m$
Lattice constants	a = 7.4347(5) Å; b = 5.6270(5) Å, c = 9.4919(5) Å and β = 90.870(6)°
Data collection	
Diffractometer	Enraf−Nonius CAD4
Radiation	λ(Mo-K_α) = 0.7107 Å
Scan mode	ω-2θ
(*hkl*) min., (*hkl*) max.	(−10,−7,−13), (10,1,0)
θ range	2−30°
Independent reflections	1263
Observed reflections	1191 [$F_O > 4\ \sigma(F_O)$]
Refinement	
Parameters	80
$R = \Sigma\|\|F_O\| - \|F_C\|\|/\Sigma\|F_O\|$	0.0455 [0.044 for $F_O > 4\ \sigma(F_O)$]
$Rw = [\Sigma\|\|F_O\| - \|F_C\|\|^2/\Sigma w\|F_O\|^2]^{1/2}$	0.1136

Table 5. Ionic coordinates and equivalent isotropic displacement factors for $K_3Sm(PO_4)_2$

Atoms	x	y	z	U_{eq}
P(1)	−0.1930(2)	1/4	0.5737(1)	0.0079(3)
P(2)	−0.2325(2)	3/4	0.0875(1)	0.0076(3)
O(1)	−0.2833(6)	1/4	0.4263(5)	0.0117(8)
O(2)	0.0102(7)	1/4	0.5994(5)	0.0242(13)
O(3)	0.2484(4)	−0.0262(6)	0.3426(3)	0.0139(6)
O(4)	−0.1755(6)	3/4	−0.0677(5)	0.0120(9)
O(5)	0.4349(6)	1/4	−0.1010(5)	0.0181(10)
O(6)	−0.1536(4)	−0.0260(6)	0.1612(3)	0.0137(6)
K(I)	−0.4940(1)	1/4	0.1923(1)	0.0148(3)
Sm	0.00705(3)	1/4	0.29098(3)	0.0077(2)
K(IIa)	−0.2035(2)	1/4	−0.0821(1)	0.0122(3)
K(IIb)	0.3627(2)	1/4	0.5920(1)	0.0155(3)

Experimental Section

Preparation: Single crystals of $K_3Sm(PO_4)_2$ were obtained by solid-state reaction of K_2CO_3, $(NH_4)_2HPO_4$, Sm_2O_3, and KF in a 3:4:1:10 molar ratio. After grinding, the mixture was heated at 400°C for 4 h, then at 900°C for 6 h, and was finally allowed to

Table 6. Bond lengths (Å) and selected angles (°) in $K_3Sm(PO_4)_2$

P(1)−O(2)	1.532(5)	O(2)−P(1)−O(2)	106.2(2)	P(2)−O(5)	1.513(5)
P(1)−O(1)	1.542(5)	O(2)−P(1)−O(3)	110.3(1) × 2	P(2)−O(4)	1.539(5)
P(1)−O(3)	1.548(4) × 2	O(1)−P(1)−O(3)	110.5(2) × 2	P(2)−O(6)	1.552(4) × 2
		O(3)−P(1)−O(3)	108.8(2)		
O(4)−P(2)−O(5)	111.7(2)			K(I)−O(1)	2.699(5)
O(5)−P(2)−O(6)	109.3(1) × 2	Sm−O(6)	2.305(3) × 2	K(I)−O(4)	2.710(5)
O(4)−P(2)−O(6)	110.9(1) × 2	Sm−O(3)	2.419(3) × 2	K(I)−O(5)	2.827(5)
O(6)−P(2)−O(6)	108.5(2)	Sm−O(2)	2.453(5)	K(I)−O(2)	2.863(4) × 2
		Sm−O(4)	2.478(5)	K(I)−O(5)	2.979(2) × 2
K(IIa)−O(5)	2.691(5)	Sm−O(1)	2.529(5)	K(I)−O(6)	2.988(4) × 2
K(IIa)−O(3)	2.790(4) × 2				
K(IIa)−O(6)	2.803(4)	K(IIb)−O(2)	2.646(5)	K(I)−O(1)	2.880(1)
K(IIa)−O(4)	2.824(1) × 2	K(IIb)−O(1)	2.880(1) × 2	K(I)−O(3)	2.946(4) × 2
K(IIa)−O(6)	3.043(4)	K(IIb)−O(5)	2.954(5)	K(I)−O(6)	3.099(4) × 2
K(IIa)−O(4)	3.138(5)	K(IIb)−O(1)	3.086(5)	K(I)−O(3)	3.205(4) × 2

cool to room temperature at a rate of 10°C/h. Small needles were separated from the flux by repeated washing in hot water.

X-ray Data Collection: The X-ray diffraction intensities from a single crystal ($0.05 \times 0.1 \times 0.12$ mm^3) were collected using a Nonius CAD4 four-circle diffractometer with graphite-monochromated Mo-K_α radiation ($\lambda = 0.7107$ Å). The unit cell parameters were determined by a least-squares fit of 25 randomly located reflections between 22° and 32° in 2 θ. The total sphere of reflection with index ranges $-10 \leq h \leq 10$, $-7 \leq k \leq 1$, $-3 \leq l \leq 0$ was measured and one standard reflection (−4 1 1) was monitored hourly. No absorption correction was applied ($R_\mu = 0.65$).

The experimental details are given in Table 4. The structure calculations were performed with the SHELXS-86[22] and SHELXL-93[23] programs. The atomic positions, selected bond lengths and angles are reported in Tables 5 and 6, respectively.

Raman Spectroscopy: The Raman spectra were recorded with a DILOR Z24 spectrometer. An argon laser (Coherent Innova 90.3) was used for the excitation: radiation of the wavelength 514.5 nm was chosen since the possible luminescence lines from samarium are weak and appear outside of the spectral range where the Raman signals appear. The spectral width (full-width at half-maximum) was less than 6 cm^{-1} and the error in the line positions was less than 1 cm^{-1}. The measurements were made at room temperature under a microscope (in the back-scattering geometry) with a × 50 objective with a long working distance. This was performed on micrometric samples (typically less than 0.1 mm in length) fixed on a goniometer head and suitably orientated for polarization analysis. The orientations were deduced from the growth faces of the crystals, which were needle-shaped with diamond-shaped bases. For the structure deriving from trigonal glaserite, the needle axis corresponds to the *c* direction and so to [100] of the monoclinic cell of $K_3Sm(PO_4)_2$.

Infrared Spectroscopy: The infrared absorption spectra in KBr pellets were obtained on a Perkin−Elmer FT-IR 1000 PC spectrophotometer in the range 4000−200 cm^{-1} with 4 cm^{-1} spectral resolution.

[1] R. Salmon, C. Parent, A. Berrara, R. Brochu, A. Daoudi, M. Vlasse, G. Le Flem, *C. R. Acad. Sci. Paris* **1975**, *280*, 805.
[2] R. Salmon, C. Parent, A. Daoudi, G. Le Flem, *Rev. Chim. Minér.* **1975**, *12*, 448.
[3] M. Vlasse, R. Salmon, C. Parent, *Inorg. Chem.* **1976**, *15*, 1440.
[4] R. Salmon, C. Parent, G. Le Flem, M. Vlasse, *Acta Cryst.* **1976**, *B32*, 2799.
[5] R. Salmon, C. Parent, G. Le Flem, M. Vlasse, *Mater. Res. Bull.* **1978**, *13*, 439.
[6] R. Salmon, C. Parent, G. Le Flem, *C. R. Acad. Sci. Paris* **1978**, *286*, 365.
[7] R. Salmon, C. Parent, G. Le Flem, M. Vlasse, *Mater. Res. Bull.* **1979**, *14*, 85.
[8] V. Aefremov, P. P. Melnikov, L. N. Komissarova, *Rev. Chim. Minér.* **1985**, *22*, 666.
[9] C. Parent, R. Salmon, G. Demazeau, G. Le Flem, *J. Solid State Chem.* **1980**, *35*, 83.
[10] J. Zah Letho, P. Houenou, R. Eholie, *C. R. Acad. Sci. Paris* **1988**, *307*, 1177.
[11] H. Y. P. Hong, S. R. Chinn, *Mat. Res. Bull.* **1976**, *11*, 421.
[12] K. Okada, J. Ossaka, *Acta Cryst.* **1980**, *B36*, 919.
[13] *International Tables for Crystallography*, vol. 1, Kynoch Press, Birmingham, **1974**.
[14] W. H. Baur, A. A. Khan, *Acta Cryst.* **1972**, *17*, 1195.
[15] J. A. McGinnety, *Acta Cryst.* **1972**, *B28*, 2845.
[16] K. Nakamoto, *Infrared Spectra of Inorganic and Coordination Compounds*, Wiley Interscience, New York, **1986**.
[17] H. Poulet, J. P. Mathieu, *Spectres de Vibration et Symétrie des Cristaux*, Gordon and Breach, Paris, **1970**; G. Turrel, *Infrared and Raman Spectra of Crystals*, Academic Press, London and New York, **1972**; B. Schrader (Ed.), *General Survey of Vibrational Spectroscopy in Infrared and Raman Spectroscopy*, VCH Verlagsgesellschaft mbH, Weinheim, **1995**, and references therein.
[18] M. Barj, G. Lucazeau, P. Colomban, Proceedings of the 8th International Conference on Raman Spectroscopy (6−11 Sept. **1982**, Bordeaux, France, Eds.: J. Lascombes, P. V. Huong), John Wiley & New York, **1982**, p. 461.
[19] M. Maczka, *Eur. J. Solid State Inorg. Chem.* **1996**, *T.33*, 783.
[20] R. F. Klevtsova, P. V. Klevtsov, *Kristallografiya* **1970**, *15*, 953.
[21] M. Barj, H. Pertuis, P. Colomban, *Solid State Ionics* **1983**, *11*, 157.
[22] *SHELXS-86*, in Crystallographic Computing 3 (Eds.: G. M. Sheldrick, C. Kruger, R. Goddard), Oxford University Press, **1985**.
[23] G. M. Sheldrick, *SHELXL-93: Program for the Refinement of Crystal Structures*, University of Göttingen, Germany, **1993**.

Received February 15, 1999

Received February 15, 1999
[99046]